Photoelectron Spectra and Electronic Structures of the Radiosensitizer Nimorazole and Related Compounds

ARTICLE *in* THE JOURNAL OF PHYSICAL CHEMISTRY A · SEPTEMBER 2015

Impact Factor: 2.69 · DOI: 10.1021/acs.jpca.5b05950

10 AUTHORS, INCLUDING:

Oksana Plekan

Sincrotrone Trieste S.C.p.A.

95 PUBLICATIONS **1,011** CITATIONS

SEE PROFILE

Marawan Ahmed

University of Alberta

22 PUBLICATIONS **44** CITATIONS

SEE PROFILE

Jonathan White

University of Melbourne

212 PUBLICATIONS **1,952** CITATIONS

SEE PROFILE

Kevin Charles Prince

Sincrotrone Trieste S.C.p.A.

479 PUBLICATIONS **7,033** CITATIONS

SEE PROFILE

THE JOURNAL OF PHYSICAL CHEMISTRY A

Article

pubs.acs.org/JPCA

Photoelectron Spectra and Electronic Structures of the Radiosensitizer Nimorazole and Related Compounds

Linda Feketeová,[*,†,‡,§] Oksana Plekan,[∥] Mayanthi Goonewardane,[⊥] Marawan Ahmed,[⊥] Abigail L. Albright,[†] Jonathan White,[†] Richard A. J. O'Hair,[†,‡] Michael R. Horsman,[#] Feng Wang,[⊥] and Kevin C. Prince[∥,⊥]

[†]School of Chemistry and Bio21 Institute of Molecular Science and Biotechnology, The University of Melbourne, 30 Flemington Road, 3010 Parkville, Victoria, Australia

[‡]ARC Centre of Excellence for Free Radical Chemistry and Biotechnology, Parkville, Victoria 3010, Australia

[§]Institut de Physique Nucléaire de Lyon, Université Claude Bernard Lyon1, Université de Lyon, CNRS/IN2P3 UMR 5822, 43 Bd du 11 novembre 1918, 69622 Villeurbanne Cedex, France

[∥]Elettra-Sincrotrone Trieste, in Area Science Park, 34149 Basovizza, Trieste, Italy

[⊥]Molecular Model Discovery Laboratory, Department of Chemistry and Biotechnology, Faculty of Science, Engineering and Technology, Swinburne University of Technology, 3122 Hawthorn, Victoria, Australia

[#]Department of Experimental Clinical Oncology, Aarhus University Hospital, Nørrebrogade 44, 8000 Aarhus C, Denmark

Supporting Information

ABSTRACT: Soft X-ray photoelectron spectroscopy has been used to investigate the radiosensitizer nimorazole and related model compounds. We report the valence and C, N, and O 1s photoemission spectra and K-edge NEXAFS spectra of gas-phase nimorazole, 1-methyl-5-nitroimidazole, and 4(5)-nitroimidazole in combination with theoretical calculations. The valence band and core level spectra are in agreement with theory. We determine the equilibrium populations of the two tautomers in 4(5)-nitroimidazole and find a ratio of 1:0.7 at 390 K. The NEXAFS spectra of the studied nitroimidazoles show excellent agreement with spectra of compounds available in the literature that exhibit a similar chemical environment. By comparing 1-methyl-5-nitroimidazole (single tautomer) with 4(5)-nitroimidazole, we are able to disentangle the photoemission and photoabsorption spectra and identify features due to each single tautomer.

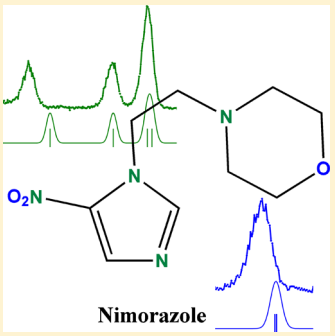

INTRODUCTION

Radiosensitizers are used in radiotherapy to enhance the killing of tumor cells by radiation, while exerting a lesser effect on normal tissues. Nimorazole, one of the compounds in this investigation, has been tested clinically and is in medical use in radiotherapy in Denmark (following the DAHANCA 5 clinical trial)[1] to enhance tumor control of radioresistant hypoxic tumors in head and neck cancers with encouraging results.[2] Nimorazole belongs to the group of radiosensitizers implemented particularly in the treatment of radioresistant hypoxic cells, that is, tumor cells deprived of oxygen, and are denoted "electron-affinic" because they have shown a relationship between the efficiency of sensitization and the electron affinity.[3−5] Nonetheless, the detailed mechanism of the actual radiosensitization remains unknown. A working hypothesis is that nitroimidazole-based radiosensitizers, including nimorazole, undergo complex redox reactions inside the cells that are deprived of oxygen, and that the nitroimidazole ring facilitates reduction via the formation of radical anions.[4] Therefore, new potential radiosensitizers were suggested in the recent work of Ramalho et al. on the basis of the calculation of adiabatic and vertical electron affinities of nitrofurans and nitroimidazoles in solution.[6]

Gas-phase studies of compounds related to nitroimidazole are limited to the pioneering photoelectron spectroscopy (PES) work of Kajfež et al.,[7] PES and mass analyzed ion kinetic energy spectra (MIKE) study by Jimenez et al.,[8] and a recent nanosecond energy-resolved spectroscopy study by Yu and Bernstein.[9,10] Recently, a mass spectrometry study of radiosensitizers, including nimorazole, showed the potential for utilizing electrospray ionization ion trap mass spectrometry to investigate the formation of radical anions of nitroimidazolic radiosensitizers and related model compounds.[11] The subsequent work of Tanzer et al. reported the reactions in the gas phase of nitroimidazole and methylated nitroimidazole induced by attachment of free electrons and showed that methylation of nitroimidazole at the N1 site completely blocks the rich chemistry induced by low energy (<2 eV) electrons.[12] These results highlight the importance of understanding the physical

Received: June 22, 2015
Revised: August 25, 2015

DOI: 10.1021/acs.jpca.5b05950
J. Phys. Chem. A XXXX, XXX, XXX−XXX

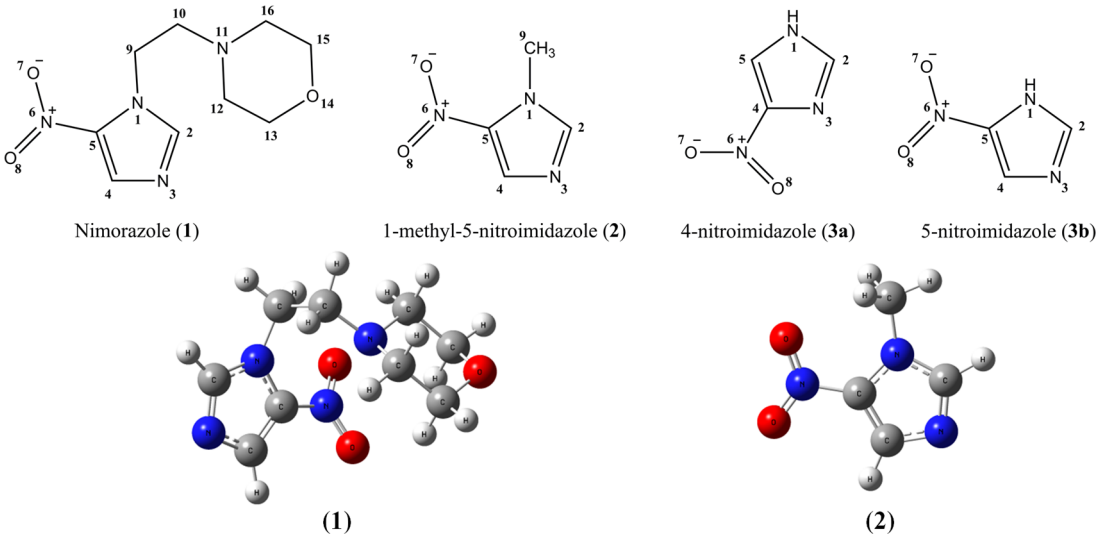

Figure 1. Structures of nitroimidazole compounds in this study.

and chemical properties of these compounds in order to aid the development of nitroimidazole based radiosensitizers in tumor radiation therapy.

The study of the electronic structure of isolated nitroimidazole compounds by soft X-ray PES has been limited to the binding energy range of outer valence orbitals.[7,8] In order to increase our knowledge of the electronic properties of radiosensitizers, the current work investigates the X-ray photoelectron spectroscopy (XPS) and near edge X-ray absorption fine structure (NEXAFS) of the radiosensitizer nimorazole (**1**) and the model compounds 1-methyl-5-nitroimidazole (1Me5NI) (**2**) and 4(5)-nitroimidazole (**3**), see Figure 1. XPS and NEXAFS are very sensitive to the chemical environment of the ionized or excited atom, and therefore characteristic of the electronic structure of nitroimidazole and its derivatives. Additionally, high-resolution core-level spectroscopy has been shown to be a very effective way of determining the gas-phase tautomeric population of molecular compounds.[13−15] 4-nitroimidazole (4NI) (**3a**) and 5-nitroimidazole (5NI) (**3b**) are regioisomers that differ in the position of the H atom on either of the two N atoms within the imidazole ring. It has been reported that 5NI is more stable in the gas phase, while 4NI is favored in the crystalline state.[16] In substituted nitroimidazoles, such as (**2**) and (**1**), tautomerism does not occur. On the basis of the advantages of XPS as a quantitative method, the tautomeric equilibrium of 4(5)-nitroimidazole in the gas phase can be probed. Moreover, the present gas-phase studies will be important in investigating the photoelectron spectra of nitroimidazoles in solution that has became possible with the development of liquid microjets for photoelectron spectroscopy applications.[17,18] Quantum mechanical calculations have been performed in order to aid the interpretation of the valence and core level spectra.

MATERIALS AND METHODS

Materials. Nimorazole (**1**) was provided by the Department of Experimental Clinical Oncology, Aarhus University Hospital and was used as received. 1-Methyl-5-nitroimidazole (**2**) was prepared by the method of Groziak and Ding.[19] 4(5)-Nitroimidazole, consisting of tautomers **3a** and **3b**, was purchased from Alfa Aesar (purity 97%).

Methods. The measurements were performed at the Gas-Phase Photoemission beamline, Elettra Trieste,[20] using the previously described apparatus and calibration methods.[21−23] The samples were evaporated at temperatures of 337 K (**1**), 299 K (**2**), and 390 K (**3**) and checked for signs of thermal decomposition by looking for spectral changes as a function of time, discoloration after heating, and so forth. No evidence was found for the decomposition of the compounds.

Theoretical Calculations. The computational methods have been described previously,[24,25] and will not be discussed here in detail. The geometries of nimorazole (**1**), 1Me5NI (**2**), 4NI (**3a**), and 5NI (**3b**) were taken from ref 11. In the case of nimorazole, for the outer valence spectra the two lowest energy conformers were considered, while for the core ionization only the lowest energy conformer was studied. The outer valence vertical ionization energies were calculated using the outer valence Green function OVGF/6-311+G** model.[26−28] For **2** and **3**, the outer valence vertical ionization energies were also calculated using the statistical averaging of (model) orbital potentials SAOP/et-pVQZ model.[29]

Core ionization energy calculations were performed by applying the ΔE_{KS} method.[30] The ΔE_{KS} method determines the difference in the total Kohn−Sham energies between the core-ionized cation and the neutral parent molecule using the (PW86-PW91)/et-pVQZ model, thereby taking account of the core hole relaxation effects.[25] The calculations of the binding energy (ionization potential, IP) spectra, that is, ΔE_{KS} and SAOP/et-pVQZ calculations were carried out using the Amsterdam Density Functional (ADF) computational chemistry program.[31−33] Other calculations were performed with the Gaussian 09 computational chemistry program.[34]

RESULTS AND DISCUSSION

Geometric Properties of the Compounds. As shown by the structures in Figure 1, nimorazole (**1**) has three single bonds that link the pentagonal and hexagonal rings, N11−C10−C9−N1, and rotations around these single C−C bonds (and the N6−C5 bond) produce a number of local minimum energy structures of different conformers on the potential energy surface. In this study, the global minimum structure of nimorazole (**1**) is considered. The calculated geometric properties of the nimorazole (**1**), 1Me5NI (**2**), 4NI (**3a**), and

DOI: 10.1021/acs.jpca.5b05950
J. Phys. Chem. A XXXX, XXX, XXX−XXX

5NI (**3b**), using M062*x*/6-311+G(d,p),[11] are compared to the previously reported calculated structures for 4NI and 5NI,[35] and the experimentally determined crystal structure of 4NI[36] in Supporting Information Table S1. The nitroimidazole ring perimeter R_5 remains almost unchanged for all compounds, which indicates that the substitution of H at the N1 position of the ring by the methyl group in 1Me5NI, as well as by the side chain of the nimorazole, do not appreciably perturb the pentagonal nitroimidazolic ring. The lengths of the bonds within the nitroimidazole rings of the different compounds also do not change significantly. The agreement with the reported crystallography data for 4NI shown in Supporting Information Table S1, as well as with the earlier computational study of 4NI and 5NI by Cho et al., is excellent.[35,36]

Valence Band Spectra. Figure 2 compares the measured and simulated vertical ionization spectra of the nitroimidazoles in the outer valence region. The OVGF model used in the simulation reproduces the major peaks of the experiment for the three compounds. The energy gaps between the two clusters of peaks separated at approximately 13 eV reduces as the substituted groups at N1 become larger.

The complete calculated vertical ionization potentials of 1Me5NI, 4(5)-nitroimidazole and nimorazole, respectively, together with the experimental data and other data (where available) are summarized in Supporting Information Tables S2, S3, and S4. The valence ionization potentials of 1Me5NI, 4NI, and 5NI have been calculated within the SAOP and OVGF models and, as seen in Supporting Information Tables S2 and S3, the agreement between these two models improves at larger binding energy, as observed previously.[24] The SAOP model severely underestimates the first ionization potential of all compounds but the agreement in the inner valence space apparently improves.

Figure 2a shows the experimental and simulated valence ionization spectra of 1Me5NI, and the first six orbitals in the 9–13 eV region (A–D) are in good agreement, see also Supporting Information Table S2. There is an energy gap in the density of states between the outermost six ionic states and the seventh ionic state (E). The OVGF calculation is able to produce very accurate outer valence ionization potentials compared to the experiment, if the ionization process is sufficiently fast to satisfy the vertical ionization assumption (ignoring the relaxation effects) and the ionization process is dominated by one electron ionization process that is indicated by the spectroscopic pole strength (SP > 0.85). For (C_s point group symmetry) calculations, the seventh valence ionization level, that is, orbital 3A″, shows nearly larger than 1 eV discrepancy between the calculation and the measurement. The OVGF method predicted that IP for this ionization is 14.6 eV but experimentally it is observed at 13.7 eV (E). However, the spectroscopic pole strength of this ionization is 0.87, which is very close to the one-electron approximation break down point, implying that the ionization of this state (3A″) may be dominated by many-body effects. As indicated by Danovich et al.,[37] 40–60% of the n-type orbital reorganization within the OVGF AM1 calculations exceeding 1 eV for pyridine derivatives is caused by orbital-relaxation effects. That the previous experiment[8] was unable to make the measurement at this state may also indicate the process is complex. Similarly, the states of 4(5)-nitroimidazole isomers (below) also suffer large discrepancies between the measurements and the OVGF calculations, indicating a possible breakdown of approximations

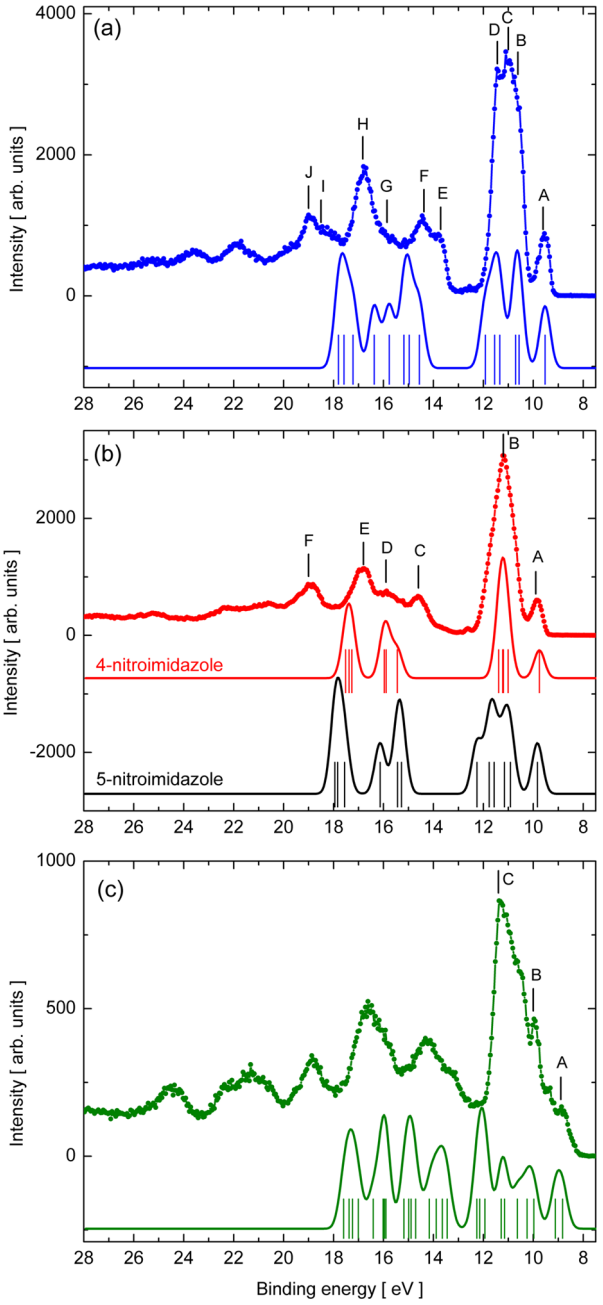

Figure 2. Valence ionization spectra of (a) 1-methyl-5-nitroimidazole, (b) 4(5)-nitroimidazole, and (c) nimorazole. Letters mark the positions of resonances. Dotted lines, experiment; full lines, theory based on the OVGF/6-311+G(d,p) level with FWHMs 0.5 eV; vertical lines, theoretical histograms.

in the model. More detailed studies, both theory and experiment, would be needed.

The first peak in the spectrum of 4(5)-nitroimidazole (Figure 2b, A) is assigned to a single state, the highest occupied molecular orbital (HOMO), while the second (B) is assigned to a band of five states. The energy of the first peak is in a good agreement with the previous measurement,[8] whereas that of the second one differs by 300 meV. This difference is attributed to the different cross sections of the constituent ionic states at 100 eV photon energy, compared to 21.2 eV used in the previous study, which may shift the centroid of the peak. At first glance, the experimental valence ionization spectrum of 4(5)-nitro-

DOI: 10.1021/acs.jpca.5b05950
J. Phys. Chem. A XXXX, XXX, XXX–XXX

imidazole appears to agree well with the simulated spectrum of 4NI, see Figure 2b. However, a close inspection of the experimental data shows that the second most intense peak at 11.1 eV (B) is broader than expected by the simulation for 4NI. The simulated 5NI spectrum also shows a peak in this region, though it is much broader than the experimental peak. This observation of a peak that is intermediate in width between the two tautomers, 4NI and 5NI, suggests the spectrum is a mixture. The presence of both tautomers in the gas phase has been noted previously in the work of Jimenez et al.,[8] who concluded the dominant form was 5NI.

As in the case of 1Me5NI, neither the calculations for 4NI nor for 5NI correctly predict the binding energy of the seventh state: experimentally it is at 14.6 eV (C), but predicted to be at 15.5 (4NI) or 15.3 (5NI) eV (Supporting Information Table S3). We do not have a definitive explanation for this discrepancy but suggest that the peak at 14.6 eV may be due to an excited final state, or satellite. As above, the spectroscopic pole strength of the 27A states of 4NI and 5NI, and the 30A state of 1Me5NI vary from 0.85 to 0.88, lower than the average, which may again indicate the breakdown of the independent particle approximation in the calculation, and the presence of satellites. The theoretical 5NI spectrum in Figure 2b shows six orbitals in the region 9−13 eV as in the case of 1Me5NI (Figure 2a), thus a substitution of H at the N1 position of 5NI by a CH_3 group in 1Me5NI causes only a small perturbation. This is evident in the small shifts of the theoretical energies of these orbitals for the two compounds, 1Me5NI and 5NI. The width of this band in the 10−13 eV region for 1Me5NI in Figure 2a also supports the presence of the two tautomers, 4NI and 5NI, in the experimental spectrum in Figure 2b.

The density of states for nimorazole in Figure 2c is high, but the calculated valence ionization spectrum agrees well with the experimental spectrum. The four states predicted by the theory at around 12 eV appear to be higher in energy in comparison with the experimentally observed band peaking at 11.4 eV (C, see Supporting Information Table S4).

Core 1s Photoemission Spectra. The experimental C 1s photoemission spectra of 1Me5NI, 4(5)-nitroimidazole and nimorazole are shown in Figure 3a−c, respectively, together with spectra predicted by the theory based on the PW86x/PW91c/et-pVQZ level, broadened with FWHM 0.5 eV. The positions of the maxima are summarized in Table 1. The vertical lines depict the theoretical energies.

In Figure 3a, the experimental spectrum of 1Me5NI nicely matches the calculated one. To align the simulated and experimental spectra, a small fixed shift of +0.15 eV was applied. The integral intensity of the two experimental peaks for 1Me5NI is 3:1, as expected from the stoichiometry.

The experimental C 1s photoemission spectrum of 4(5)-nitroimidazole in Figure 3b (red dotted line) shows that the spectrum cannot be explained in terms of the presence of only one tautomer.[8,16] Instead, the spectrum can best be fitted using a ratio of tautomeric populations of 1:0.70 for 4NI/5NI (blue line). The fit was performed by assuming that all six peaks have Gaussian profiles but variable widths and that for each tautomer the integrated intensities of each peak for a given tautomer were equal. The Gaussian function approximates the Franck−Condon envelope, which width depends on which vibrations are excited. The theoretically predicted C 1s core ionization potentials matched the experiment without a shift of the energy within 0.01 eV. This fit of the experimental data with a ratio of populations of 1:0.70 for 4NI/5NI shows that both tautomers

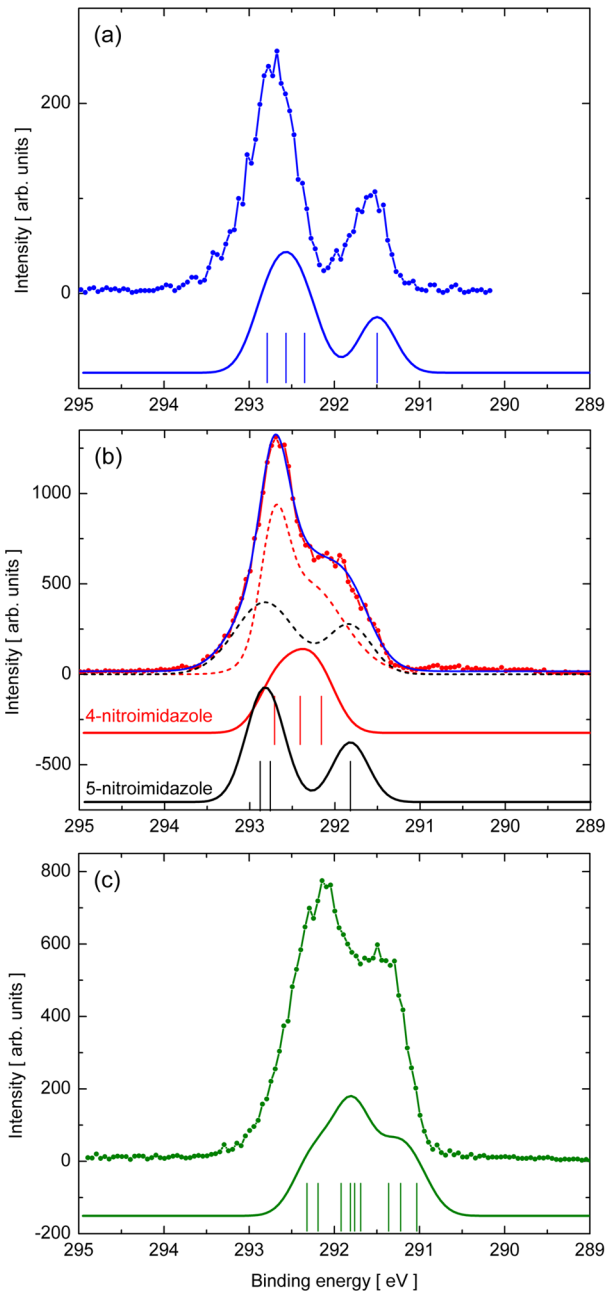

Figure 3. C 1s photoemission spectra of (a) 1-methyl-5-nitroimidazole, (b) 4(5)-nitroimidazole, and (c) nimorazole. Dotted lines, experiment; full lines, theory based on the PW86x/PW91c/et-pVQZ model with FWHMs 0.5 eV; vertical lines, theoretical histograms. Simulation of C 1s photoemission spectrum of 4(5)-nitroimidazole in panel (b) in blue includes a contribution of 4NI (dashed red) and 5NI (dashed black) with population ratio 1:0.70.

are present in the gas-phase with a slightly higher population of the 4NI tautomer. It corresponds to a difference in free energy of only 1.1 kJ/mol at 390 K. This finding finally clarifies the ambiguity raised in the gas-phase experiments on tautomeric 4(5)-nitroimidazole,[7,8,16] regarding which tautomer is dominant, and contradicts the conclusion of Jimenez et al.,[8] although we note that the temperature of 4(5)-nitroimidazole in their study was not reported. Therefore, it would be of interest to investigate the ratio of population of 4NI and 5NI at different temperatures. While the presence of both tautomers is qualitatively apparent in the valence ionization spectrum

DOI: 10.1021/acs.jpca.5b05950
J. Phys. Chem. A XXXX, XXX, XXX−XXX

Table 1. Experimental and Calculated C 1s Core Ionization Potentials in eV of 4(5)-Nitroimidazole, 1Me5NI, and Nimorazole (the Most Stable Conformer)[a]

	1Me5NI		4NI	5NI	nimorazole	
expt.	expt.	ΔE_{ks}	ΔE_{ks}	ΔE_{ks}	expt.	ΔE_{ks}
292.6	291.6	C4 291.50	C5 292.16	C4 291.83	291.4	C4 291.03
293.1	292.7	C2 292.35	C4 292.41	C2 292.77	292.1	C16 291.22
293.4		C5 292.57	C2 292.71	C5 292.89		C12 291.36
		C9 292.79				C15 291.69
						C10 291.76
						C13 291.81
						C2 291.92
						C5 292.19
						C9 292.32

[a]The core ionization potentials are calculated using the ΔE_{ks} at the PW86x/PW91c/et-pVQZ level of theory.

shown in Figure 2b and the C 1s core ionization spectrum depicted in Figure 3b, the high-resolution spectroscopy data and theoretical calculations constitute a strong analytical tool to address such questions, and quantify the results. The C 1s core ionization spectrum of 1Me5NI shown in Figure 3a confirms the presence of 4NI and 5NI in the spectrum in Figure 3b because the splitting in the spectrum of 1Me5NI is large and also appears in the width of the spectrum of 4(5)-nitroimidazole (Figure 3b). The extra carbon due to the CH_3 group in 1Me5NI overlaps the stronger peak.

The simulated C 1s core ionization spectrum of nimorazole depicted in Figure 3c consists of peaks with nine ionization potentials, associated with the nine carbon atoms in the molecule, and little fine structure can be resolved. However, the overall bandwidth and shape of the simulated spectrum matches the experimental spectrum. To align the simulated spectrum of nimorazole with the experimental data a small shift of +0.25 eV was necessary.

Figure 4 shows the N 1s experimental and simulated core ionization spectra for 1Me5NI, 4(5)-nitroimidazole, and nimorazole, and the positions of the maxima are summarized in Table 2. While the ring amino and imino nitrogen atoms (N1 and N3) have very similar energies, the 4(5)-nitroimidazole peak at 412 eV due to N6 (Figure 4b) is predicted to have slightly different energies for 4NI and 5NI. Comparison of this peak with the case of 1Me5NI in Figure 4a shows clearly that the peak in the 4(5)-nitroimidazole is substantially broader than in 1Me5NI, which again implies both tautomers are present in 4(5)-nitroimidazole. Assuming the ratio of 4NI/5NI found earlier, 1:0.70, the combination of theoretically predicted N 1s spectra leads to a peak shape that nicely matches the shape of the peak in the experiment, however theory underestimates the position of this maximum by 0.6 eV. The N 1s spectrum of nimorazole (Figure 4c) has an extra contribution due to the additional nitrogen in the morpholine ring. This contribution is part of the first peak in the spectrum at 404.8 eV slightly shifted by 0.1 eV from the experiment. The ratio of integrated intensity of the three experimental peaks for nimorazole is 1:1:1.9, which is in a good agreement with the expected stoichiometric ratio.

Experimental and simulated O 1s core ionization spectra for 1Me5NI, 4(5)-nitroimidazole, and nimorazole are shown in Figure 5a–c, respectively. The positions of the maxima are summarized in Table 3. Modeling the experimental spectrum of 4(5)-nitroimidazole with a population ratio of 1:0.70 for 4NI/5NI using the calculated energies predicts the O 1s peak is broader than the spectrum of 1Me5NI by 0.2 eV. The experimental relative broadening of the 4(5)-nitroimidazole O 1s peak is 0.15 eV, thus, in good agreement. The theory predicts the O 1s binding energy of nimorazole is 0.35 eV lower than 1Me5NI and 4(5)-nitroimidazole at 538.25 eV. Experimentally the O 1s peak of nimorazole is lower than that of 1Me5NI but is at the same energy as for 4(5)-nitroimidazole. Thus, the agreement is partial in this case.

All of the O 1s experimental core ionization spectra in Figure 5 show a broad maximum at around 542 eV (about 3.5 eV from the main peak), assigned to a $\pi-\pi^*$ shakeup.

K-edge NEXAFS spectra. Figures 6, 7, and 8 present the C, N, and O K-edge NEXAFS spectra, respectively of 1Me5NI (blue), 4(5)-nitroimidazole (red), and nimorazole (green). The positions of the maxima are summarized in Table 4. The C and N 1s K edge spectra of some solid state imidazoles were measured by Apen et al.[38] and the N K edge spectra of some solid state five-ring heterocycles including 2-methyl-4-nitroimidazole were measured by Leinweber et al.[39] We assign the NEXAFS spectra on the basis of these and other reference compounds.[40]

Imidazole is aromatic and has two formal double bonds, which in reality are delocalized, so that two unoccupied π^* orbitals are expected within a simplified one-electron model. For the C K edge spectra (Figure 6), the first two resonances of 1Me5NI at 285.3 and 286.4 eV are assigned to transitions to $1\pi^*$ and $2\pi^*$ resonances, as in the case of imidazole. These structures were unresolved in the solid state and low-resolution gas-phase spectra, although a shoulder was present.[38] The peaks differ in energy by 1.1 eV, which is also the difference in the experimental binding energy between the C2 peak and the C4 plus C5 peak. This suggests that the π^* orbitals have similar one-electron energies and that the separation is mostly determined by the difference in core level binding energy. The third peak at 287.9 eV is assigned in part to C9 transitions to 3p Rydberg states, as the methyl group is expected to have resonances similar to methane, for which this transition is at 288.0 eV.[41] However, other transitions are also possible. The other states at 288.7 and 289.1 eV are assigned to transitions of the ring carbon atoms to π^* and Rydberg transitions of the aromatic system but without calculations it is difficult to give a precise assignment. The broad peaks at 293.8 and 301.2 eV are due to transitions to σ^* states.

The assignments for 4(5)-nitroimidazole are based on those of 1Me5NI. We expect the 5-nitroimidazole tautomer to have a spectrum very similar to 1Me5NI (less any structure due to the methyl group), while the other tautomer may have a different spectrum. In Table 4, we see that peaks A, C, E, F, and G are

DOI: 10.1021/acs.jpca.5b05950
J. Phys. Chem. A XXXX, XXX, XXX−XXX

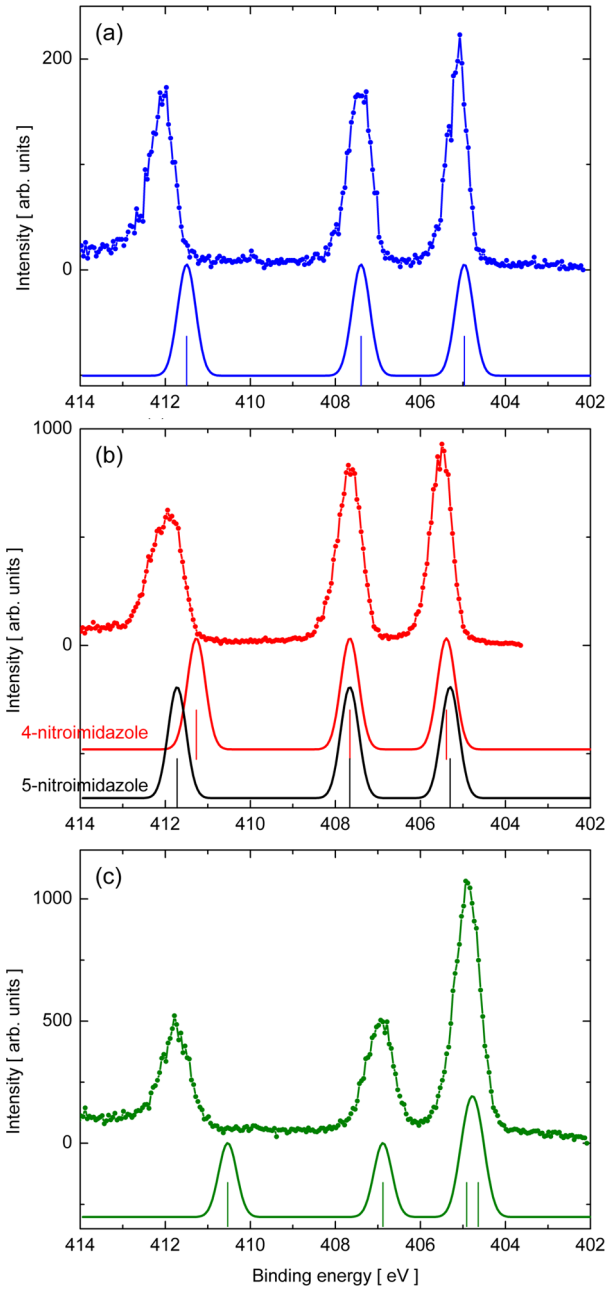

Figure 4. N 1s photoemission spectra of (a) 1-methyl-5-nitroimidazole, (b) 4(5)-nitroimidazole, and (c) nimorazole. Dotted lines, experiment; full lines, theory based on the PW86x/PW91c/et-pVQZ level with FWHMs 0.5 eV; vertical lines, theoretical histograms.

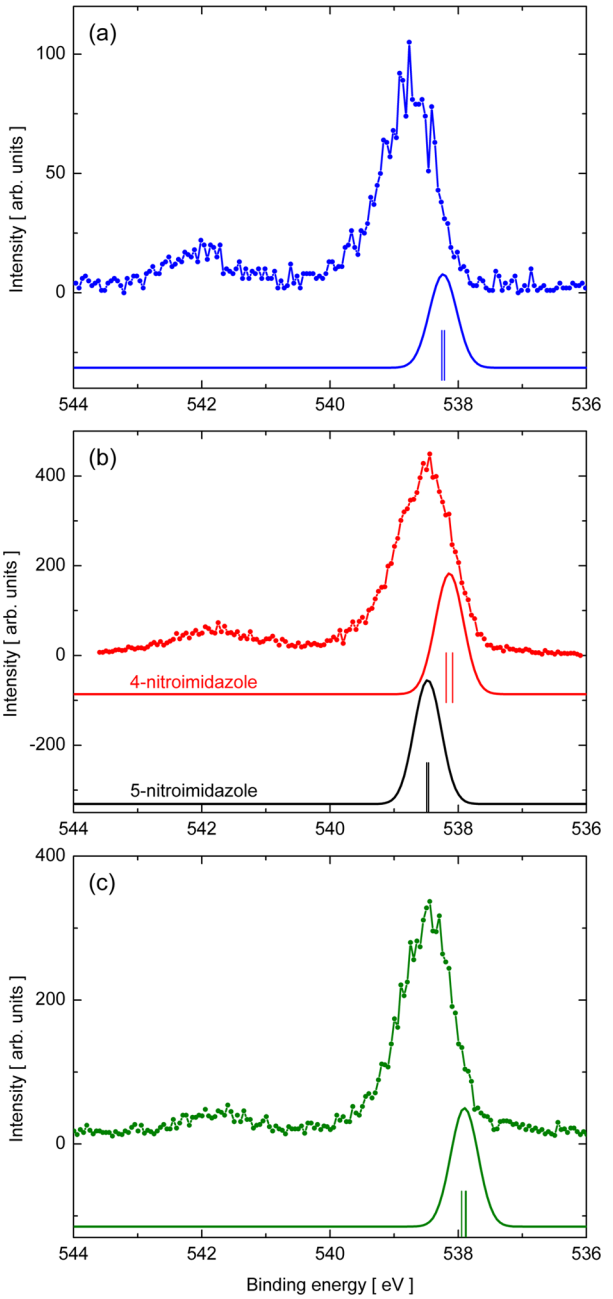

Figure 5. O 1s photoemission spectra of (a) 1-methyl-5-nitroimidazole, (b) 4(5)-nitroimidazole, and (c) nimorazole. Dotted lines: experiment; full lines: theory based on the PW86x/PW91c/et-pVQZ level with FWHMs 0.5 eV; vertical lines: theoretical histograms.

common to 1Me5NI and 4(5)-nitroimidazole and are thus assigned to the 5-nitroimidazole tautomer with possible

Table 2. Experimental and Calculated N 1s Core Ionization Potentials in eV of 4(5)-Nitroimidazole, 1Me5NI, and Nimorazole (the Most Stable Conformer)[a]

	1Me5NI		4NI	5NI	nimorazole	
expt.	expt.	ΔE_{ks}	ΔE_{ks}	ΔE_{ks}	expt.	ΔE_{ks}
405.5	405.1	N3 404.98	N3 405.40	N3 405.31	404.9	N3 404.65
						N11 404.92
407.6	407.4	N1 407.41	N1 407.67	N1 407.67	407.0	N1 406.89
412.0	412.1	N6 411.51	N6 411.28	N6 411.73	411.8	N6 410.54

[a]The core ionization potentials are calculated using the ΔE_{ks} at the PW86x/PW91c/et-pVQZ level of theory.

DOI: 10.1021/acs.jpca.5b05950
J. Phys. Chem. A XXXX, XXX, XXX−XXX

Table 3. Experimental and Calculated O 1s Core Ionization Potentials in eV of 4(5)-Nitroimidazole, 1Me5NI, and Nimorazole (the Most Stable Conformer)[a]

	1Me5NI		4NI	5NI	nimorazole	
expt.	expt.	ΔE_{ks}	ΔE_{ks}	ΔE_{ks}	expt.	ΔE_{ks}
538.5	538.8	O7 538.26	O7 538.09	O7 538.50	538.5	O8 537.88
		O8 538.22	O8 538.19	O8 538.47		O7 537.89
						O14 537.95
541.7	542.0	(satellite)	(satellite)	(satellite)	541.7	(satellite)

[a]The core ionization potentials are calculated using the ΔE_{ks} at the PW86x/PW91c/et-pVQZ level of theory.

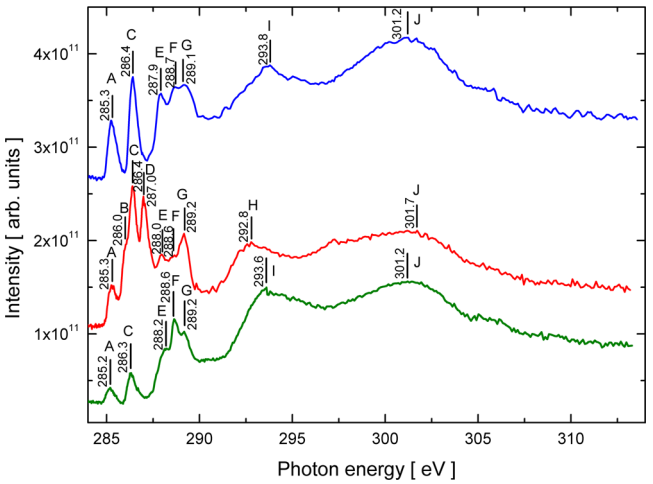

Figure 6. C K-edge NEXAFS spectra of 4(5)-nitroimidazole (red), 1-methyl-5-nitroimidazole (blue), and nimorazole (green). Letters mark the positions of resonances.

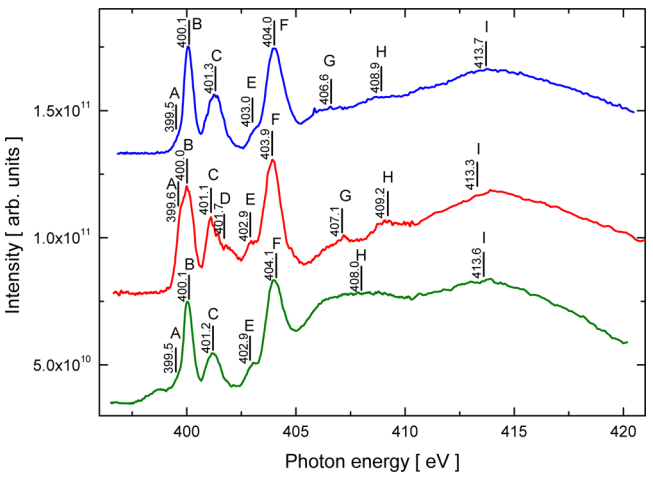

Figure 7. N K-edge NEXAFS spectra of 4(5)-nitroimidazole (red), 1-methyl-5-nitroimidazole (blue), and nimorazole (green). Letters mark the positions of resonances. Note that due to molecular nitrogen in the residual gas of the chamber, the spectral region from about 400.6 to 402 eV suffers from increased noise due to the imperfect subtraction of the strong absorption bands of this molecule.

contributions from 4-NI. Peaks B and D, however, do not appear for 1Me5NI and are therefore characteristic of 4-nitroimidazole. They are clearly C 1s to π^* transitions, whose exact assignment requires further calculations. The remaining very broad peaks are derived from transitions to σ^* states and show some variation in their energy. Peak H occurs at 1 eV lower energy than the corresponding peak I of 1Me5NI. These peaks can be interpreted as scattering resonances between C−C

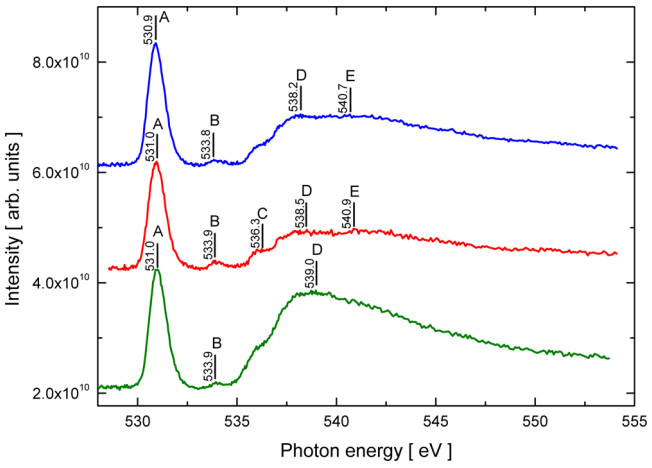

Figure 8. O K-edge NEXAFS spectra of 4(5)-nitroimidazole (red), 1-methyl-5-nitroimidazole (blue), and nimorazole (green). Letters mark the positions of resonances.

and C−N pairs of atoms and from peak J it appears the average bond length is almost the same. However, the peak arises from up to five scattering pairs with different bond lengths, phase shifts, and oscillator strengths, so some variation in resonance energy is to be expected.

Nimorazole has six more carbon atoms in saturated bonds, and the spectrum consequently shows a much stronger σ^* region compared with the lower lying π^* resonance part. Peaks A and C have the same energies as 1Me5NI (within 0.1 eV) and are assigned accordingly to the same transitions in the imidazole ring. Peak E has a similar but slightly higher energy and is more intense; we assign it to C 1s to 3p Rydberg transitions of methylene groups in the side chain of nimorazole. Peaks F and G have similar energies to 1Me5NI but again are more intense and probably originate from the resonances in the aliphatic chain. Lastly the σ^* resonances resemble those of 1Me5NI.

For the nitrogen spectra, we again begin with the 1Me5NI spectrum. The spectra of 1Me5NI and nimorazole show a weak shoulder A at 399.5 eV, which may be an electronic state, or may be the tail of the Franck−Condon envelope of the first peak; because of this ambiguity, the peaks are marked with an asterisk in Table 4. 4(5)-nitroimidazole, however, shows a strong peak at 399.6 eV and clearly has a different origin. The three compounds have in common resonances B, C, E, and F, which are identified as features characteristic of the 5-nitroimidazole molecule or moiety. The spectrum agrees approximately with the solid state spectrum of Leinweber et al.,[39] and the observed peak shifts with respect to the present results are −0.4 eV (A), −0.2 eV (B), −0.1 eV (F), and -0.7 eV (G). The solid state spectrum was much broader than our gas-

DOI: 10.1021/acs.jpca.5b05950
J. Phys. Chem. A XXXX, XXX, XXX−XXX

Table 4. Energies of Peaks (eV) in the C, N, and O K Edge NEXAFS Spectra[a]

	label	1Me5NI	4(5)-nitroimidazole	nimorazole
C 1s	A	285.3 C→1π*	285.3 C→1π*	285.2 C→1π*
	B		286.0 C→π*	
	C	286.4 C→2π*	286.4 C→2π*	286.3 C→2π*
	D		287.0 C→π*	
	E	287.9 C9→3p Rydberg	288.0	288.2 C9→3p Rydberg
	F	288.7 C→π*	288.6 C→π*	288.6 $C_{aliphatic}$→π*
	G	289.1 C→Rydberg	289.2 C→Rydberg	289.2 $C_{aliphatic}$→π*
	H		292.8 C−C,C−N→σ*	
	I	293.8 →σ*		293.6 →σ*
	J	301.2 →σ*	301.7 →σ*	301.2 →σ*
N 1s	A	399.5*	399.6	399.5*
	B	400.1 N3→π*	400.0 N3→π*	400.1 N3→π*
	C	401.3 N3→π*	401.1 N3→π*	401.2 N3→π*
	D		401.7 N1→π*	
	E	403.0	402.9	402.9
	F	404.0 N6→π*	403.9 N6→π*	404.1 N6→π*
	G	406.6	407.1	
	H	408.9	409.2	408.0
	I	413.7	413.3	413.6
O 1s	A	530.9 →2pπ*	531.0 →2pπ*	531.0 →2pπ*
	B	533.8	533.9	533.9
	C		536.3	
	D	538.2 →σ*	538.5 →σ*	539.0 →σ*
	E	540.7 →σ*	540.9 →σ*	

[a]Including the assignment of the transitions for observed resonances.

phase data, most likely due to effects such as hydrogen bonding, and the weaker peak C did not appear in their data, probably because it was obscured by this broadening. For molecules on surfaces, only two strong π resonances are observed at 399.9 and 401.35 eV[42] with broad structures at higher energies. These energies correspond well to peaks B and C.

As mentioned above, the imidazole ring has two formal π bonds and is aromatic. The strong resonance B is assigned to N1 and N3 transitions to π* states. The peak at 403.9 (±0.1) eV is attributed to a N6 1s → π* transition in the nitro group. A resonance at the same energy was observed in the N K-edge absorption spectra of gas-phase nitromethane[40] and in the 2-methyl-4-nitroimidazole solid state spectrum.[39]

The lower energy peaks of 4(5)-nitroimidazole, A and D, which are not observed for 1Me5NI, are assigned to the 4-nitroimidazole tautomer. Peak A most likely has similar orbital character to peak B in 1Me5NI and is only slightly perturbed by the 4−5 tautomerism. Similarly, peak D is probably related to peak C in 1Me5NI.

Nimorazole has an extra nitrogen N11 in the morpholine ring. A suitable reference compound may be pyrrolidine,[43] whose strongest resonances are at 401.0 and 404.5 eV. However, both of these energies overlap the assigned spectral features, B and F, so it is not possible to determine which additional features the extra nitrogen atom N11 in nimorazole adds to the spectrum.

Figure 8 shows the O 1s NEXAFS spectra for 4(5)-nitroimidazole, 1Me5NI, and nimorazole and the energies of the resonances are summarized in Table 4. The major resonance for all compounds is observed at 531.0 (±0.1 eV) eV, which is in good agreement with the O K-edge spectrum of nitromethane where the main 2pπ* transition was observed at 531.4 eV.[40] The second, less pronounced resonance at 533.9 eV appeared in the NEXAFS spectra of all three compounds investigated and was not present in the spectrum of nitromethane. Otherwise the spectra for 4(5)-nitroimidazole and 1Me5NI are very similar. The O K-edge absorption spectra of the nitromethane revealed two broad higher energy σ* derived structures at around 539 and 542 eV,[40] and some similar structures were observed in the present compounds. Despite the extra oxygen in the morpholine ring, no additional sharp oxygen resonances were found for nimorazole, which is reasonable since the extra oxygen atom is not involved in any π-bonds. The high energy σ* resonance at 539 eV has much higher intensity than 1Me5NI and 4(5)-nitroimidazole, so this is clearly the signature of the extra oxygen atom.

CONCLUSIONS

The electronic structure properties of the radiosensitizer nimorazole have been investigated, together with the model compounds 4(5)-nitroimidazole and 1Me5NI, using soft X-ray spectroscopy. Outer valence and core level photoemission and photoabsorption spectra at the C, N, and O 1s edges were recorded and compared with the theoretical spectra. The theoretical calculations of the geometric properties of all studied compounds showed that the substitutions at the N1 position of the imidazole ring do not perturb the pentagonal ring, and structure of the nitroimidazole agrees well with crystallography data. The valence level photoemission spectra of all compounds revealed two series of bands with a gap at around 13−14 eV and pointed toward the presence of tautomers in the case of 4(5)-nitroimidazole. The gas-phase tautomeric populations of 4NI and 5NI were determined from the C 1s photoemission spectrum. The high-resolution spectroscopy together with the theoretical calculations resolved the populations to have a ratio of 1:0.7 4NI/5NI at 390 K, corresponding to a free energy difference of 1.1 kJ/mol. The C and N 1s photoelectron and photoabsorption spectra of 4(5)-nitroimidazole are all consistent with the presence of two tautomers, when taking into account the spectra of the analogue 1Me5NI. The larger molecule nimorazole showed spectra in good agreement with theory.

The C, N, and O K-edge NEXAFS spectra were recorded and compared with available data of solid state imidazoles and other reference compounds related through atoms with similar chemical binding environment. The transitions characteristic to imidazole ring appeared in all three compounds with agreement in the energy required for these transitions. Radiosensitizer nimorazole showed much stronger σ* region in comparison to π* resonance part.

The spectral features of the studied compounds will be helpful in evaluating samples of unknown composition. For the case of radiosensitizers, where the composition is known, the spectral features of the gas-phase compounds will be crucial in interpreting the spectra of radiosensitizers in more complex environments of liquids and solids that will be the effort of future endeavors.

ASSOCIATED CONTENT

Supporting Information

The Supporting Information is available free of charge on the ACS Publications website at DOI: 10.1021/acs.jpca.5b05950.

DOI: 10.1021/acs.jpca.5b05950
J. Phys. Chem. A XXXX, XXX, XXX−XXX

Geometric properties of nitroimidazoles, experimental and simulated valence ionization potentials for 1Me5NI, 4- and 5-nitroimidazole, and nimorazole.
(PDF)

AUTHOR INFORMATION

Corresponding Author

*E-mail: l.feketeova@ipnl.in2p3.fr.

Notes

The authors declare no competing financial interest.

ACKNOWLEDGMENTS

The authors gratefully acknowledge support by the staff of Elettra-Sincrotrone Trieste for providing high quality light and for technical assistance on the Gas Phase beamline. We thank the ARC for support via the award of an APD (to L.F.) and through the CoE program. We thank the Department of Experimental Clinical Oncology, Aarhus University Hospital for the sample of nimorazole. M.G. was an undergraduate honours student who thanks the Swinburn University for the opportunity to work on this project. M.A. acknowledges the Swinburne University Postgraduate Research Award (SUPRA). F.W. thanks Swinburne University supercomputing (Green/gSTAR) for support on the computing facilities and the Victorian Life Sciences Computation Initiative (VLSCI) on its Peak Computing Facility at the University of Melbourne.

ABBREVIATIONS

PES, photoelectron spectroscopy
MIKE, mass analyzed ion kinetic energy spectra
XPS, X-ray photoelectron spectroscopy
NEXAFS, near edge X-ray absorption fine structure
4NI, 4-nitroimidazole
5NI, 5-nitroimidazole
1Me5NI, 1-methyl-5-nitroimidazole
SAOP, statistical averaging of model orbital potentials
OVGF, outer valence Green function
HOMO, highest occupied molecular orbital
FWHM, full width at half-maximum

REFERENCES

(1) Overgaard, J.; Hansen, H. S.; Overgaard, M.; Bastholt, L.; Berthelsen, A.; Specht, L.; Lindeløv, B.; Jørgensen, K. A Randomized Double-blind Phase III Study of Nimorazole as a Hypoxic Radiosensitizer of Primary Radiotherapy in Supraglottic Larynx and Pharynx Carcinoma. Results of the Danish Head and Neck Cancer Study (DAHANCA) Protocol 5−85. *Radiother. Oncol.* **1998**, *46*, 135−146.

(2) Overgaard, J. Hypoxic Modification of Radiotherapy in Squamous Cell Carcinoma of the Head and Neck − A Systematic Review and Meta-Analysis. *Radiother. Oncol.* **2011**, *100*, 22−32.

(3) Clarke, E. D.; Goulding, K. H.; Wardman, P. Nitroimidazoles as Anaerobic Electron Acceptors for Xanthine Oxidase. *Biochem. Pharmacol.* **1982**, *31*, 3237−3242.

(4) Edwards, D. I. Reduction of Nitroimidazoles *in Vitro* and DNA Damage. *Biochem. Pharmacol.* **1986**, *35*, 53−58.

(5) Adams, G. E.; Flockhart, I. R.; Smithen, C. E.; Stratford, I. J.; Wardman, P.; Watts, M. E. Electron-Affinic Sensitization VII. A Correlation between Structures, One-Electron Reduction Potentials, and Efficiencies of Nitroimidazoles as Hypoxic Cell Radiosensitizers. *Radiat. Res.* **2012**, *178*, AV183−AV189.

(6) Ramalho, T. C.; de Alencastro, R. B.; La-Scalea, M. A.; Figueroa-Villar, J. D. Theoretical Evaluation of Adiabatic and Vertical Electron Affinity of Some Radiosensitizers in Solution Using FEP, Ab Initio and DFT Methods. *Biophys. Chem.* **2004**, *110*, 267−279.

(7) Kajfež, F.; Klasinc, L.; Šunjić, V. Application of Photoelectron Spectroscopy to Biologically Active Molecules and their Constituent Parts IV. Methylnitroimidazoles (1). *J. Heterocycl. Chem.* **1979**, *16*, 529−531.

(8) Jimenez, P.; Laynes, J.; Claramunt, R. M.; Sanz, D.; Fayet, J. P.; Vertut, M. C.; Catalán, J.; de Paz, J. L. G.; Pfister-Guillouzo, G.; Guimon, C.; et al. The Problem of the Tautomerism of 4(5)-Nitroimidazole: A Theoretical and Experimental Study. *New. J. Chem.* **1989**, *13*, 151−156.

(9) Yu, Z.; Bernstein, E. R. Experimental and Theoretical Studies of the Decomposition of New Imidazole Based Energetic Materials: Model Systems. *J. Chem. Phys.* **2012**, *137*, 114303.

(10) Yu, Z.; Bernstein, E. R. On the Decomposition Mechanisms of New Imidazole-Based Energetic Materials. *J. Phys. Chem. A* **2013**, *117*, 1756−1764.

(11) Feketeová, L.; Albright, A. L.; Sørensen, B. S.; Horsman, M. R.; White, J.; O'Hair, R. A. J.; Bassler, N. Formation of Radical Anions of Radiosensitizers and Related Model Compounds via Electrospray Ionization. *Int. J. Mass Spectrom.* **2014**, *365*−*366*, 56−63.

(12) Tanzer, K.; Feketeová, L.; Puschnigg, B.; Scheier, P.; Illenberger, E.; Denifl, S. Reactions in Nitroimidazole Triggered by Low-Energy (0−2 eV) Electrons: Methylation at N1-H Completely Blocks Reactivity. *Angew. Chem., Int. Ed.* **2014**, *53*, 12240−12243.

(13) Zaytseva, I. L.; Trofimov, A. B.; Schirmer, J.; Plekan, O.; Feyer, V.; Richter, R.; Coreno, M.; Prince, K. C. Theoretical and Experimental Study of Valence-Shell Ionization Spectra of Guanine. *J. Phys. Chem. A* **2009**, *113*, 15142−15149.

(14) Feyer, V.; Plekan, O.; Richter, R.; Coreno, M.; de Simone, M.; Prince, K. C.; Trofimov, A. B.; Zaytseva, I. L.; Schirmer, J. Tautomerism in Cytosine and Uracil: A Theoretical and Experimental X-ray Absorption and Resonant Auger Study. *J. Phys. Chem. A* **2010**, *114*, 10270−10276.

(15) Feyer, V.; Plekan, O.; Kivimäki, A.; Prince, K. C.; Moskovskaya, T. E.; Zaytseva, I. L.; Soshnikov, D. Y.; Trofimov, A. B. Comprehensive Core-Level Study of the Effects of Isomerism, Halogenation, and Methylation on the Tautomeric Equilibrium of Cytosine. *J. Phys. Chem. A* **2011**, *115*, 7722−7733.

(16) Vokin, A. I.; Sherstyannikova, L. V.; Krivoruchka, I. G.; Aksamentova, T. N.; Krylova, O. V.; Turchaninov, V. K. Solvatochromism of Heteroaromatic Compounds: XX. 4(5)-Nitroimidazole. *Russ. J. Gen. Chem.* **2003**, *73*, 973−984.

(17) Faubel, M.; Steiner, B.; Toennies, J. P. Measurement of He I Photoelectron Spectra of Liquid Water, Formamide and Ethylene Glycol in Fast-Flowing Microjets. *J. Electron Spectrosc. Relat. Phenom.* **1998**, *95*, 159−169.

(18) Winter, B. Liquid Microjet for Photoelectron Spectroscopy. *Nucl. Instrum. Methods Phys. Res., Sect. A* **2009**, *601*, 139−150.

(19) Groziak, M. P.; Ding, H. Halogenated (Acylamino) Imidazoles and Benzimidazoles for Directed Halogen-Metal Exchange-Based Functionalization. *Acta Chim. Slov.* **2000**, *47*, 1−18.

(20) Prince, K. C.; Blyth, R. R.; Delaunay, R.; Zitnik, M.; Krempasky, J.; Slezak, J.; Camilloni, R.; Avaldi, L.; Coreno, M.; Stefani, G.; et al. The Gas-Phase Photoemission Beamline at Elettra. *J. Synchrotron Radiat.* **1998**, *5*, 565−568.

(21) Plekan, O.; Feyer, V.; Richter, R.; Coreno, M.; de Simone, M.; Prince, K. C.; Carravetta, V. Photoemission and the Shape of Amino Acids. *Chem. Phys. Lett.* **2007**, *442*, 429−433.

(22) Plekan, O.; Feyer, V.; Richter, R.; Coreno, M.; de Simone, M.; Prince, K. C.; Carravetta, V. An X-ray Absorption Study of Glycine, Methionine and Proline. *J. Electron Spectrosc. Relat. Phenom.* **2007**, *155*, 47−53.

(23) Plekan, O.; Feyer, V.; Richter, R.; Coreno, M.; de Simone, M.; Prince, K. C.; Carravetta, V. Investigation of the Amino Acids Glycine, Proline, and Methionine by Photoemission Spectroscopy. *J. Phys. Chem. A* **2007**, *111*, 10998−11005.

(24) Wickrama Arachchilage, A. P.; Wang, F.; Feyer, V.; Plekan, O.; Prince, K. C. Correlation of Electronic Structures of Three Cyclic Dipeptides with Their Photoemission Spectra. *J. Chem. Phys.* **2010**, *133*, 174319.

DOI: 10.1021/acs.jpca.5b05950
J. Phys. Chem. A XXXX, XXX, XXX−XXX

(25) Ahmed, M.; Wang, F.; Acres, R. G.; Prince, K. C. Structures of Cycloserine and 2-Oxazolidinone Probed by X-ray Photoelectron Spectroscopy: Theory and Experiment. *J. Phys. Chem. A* **2014**, *118*, 3645−3654.
(26) Cederbaum, L. S.; Domcke, W. Theoretical Aspects of Ionization Potentials and Photoelectron Spectroscopy: A Green's Function Approach. *Adv. Chem. Phys.* **1977**, *36*, 205−344.
(27) von Niessen, W.; Schirmer, J.; Cederbaum, L. S. Computational Methods for the One-Particle Green-Function. *Comput. Phys. Rep.* **1984**, *1*, 57−125.
(28) Zakrzewski, V. G.; Ortiz, J. V. Semidirect Algorithms for 3rd-Order Electron Propagator Calculations. *Int. J. Quantum Chem.* **1995**, *53*, 583−590.
(29) Schipper, P. R. T.; Gritsenko, O. V.; van Gisbergen, S. J. A.; Baerends, E. J. Molecular Calculations of Excitation Energies and (Hyper)Polarizabilities with a Statistical Average of Orbital Model Exchange-Correlation Potentials. *J. Chem. Phys.* **2000**, *112*, 1344−1352.
(30) Takahata, Y.; Wulfman, C. E.; Chong, D. P. Accurate Calculation of N1s and C1s Core Electron Binding Energies of Substituted Pyridines. Correlation with Basicity and with Hammett Substituent Constants. *J. Mol. Struct.: THEOCHEM* **2008**, *863*, 33−38.
(31) te Velde, G.; Bickelhaupt, F. M.; Baerends, E. J.; Fonseca-Guerra, C.; van Gisbergen, S. J. A.; Snijders, J. G.; Ziegler, T. Chemistry with ADF. *J. Comput. Chem.* **2001**, *22*, 931−967.
(32) Guerra, C. F.; Snijders, J. G.; te Velde, G.; Baerends, E. J. Towards an Order-N DFT Method. *Theor. Chem. Acc.* **1998**, *99*, 391−403.
(33) ADF2010; Vrije University: Amsterdam, The Netherlands.
(34) Frisch, M. J.; Trucks, G. W.; Schlegel, H. B.; Scuseria, G. E.; Robb, M. A.; Cheeseman, J. R.; Scalmani, G.; Barone, V.; Mennucci, B.; Petersson, G. A. et al. *Gaussian 09 D.01*; Gaussian, Inc.: Wallingford, CT, 2009.
(35) Cho, S. G.; Cheun, Y. G.; Park, B. S. A Computational Study of Imidazole, 4-Nitroimidazole, 5-Nitroimidazole and 4,5-Dinitroimidazole. *J. Mol. Struct.: THEOCHEM* **1998**, *432*, 41−53.
(36) De Bondt, H. L.; Ragia, E.; Blanton, N. M.; Peeters, O. M.; De Ranter, C. J. Structure of 4(5)-Nitroimidazole at 100 K. *Acta Crystallogr., Sect. C: Cryst. Struct. Commun.* **1993**, *49*, 693−695.
(37) Danovich, D. K.; Turchaninov, V. K.; Zakrzewski, V. G. OVGF AM1 Calculations on the Ionization Energies of Pyridine-Derivatives. *J. Mol. Struct.: THEOCHEM* **1990**, *209*, 77−87.
(38) Apen, E.; Hitchcock, A. P.; Gland, J. L. Experimental Studies of the Core Excitation of Imidazole, 4,5-Dicyanoimidazole, and s-Triazine. *J. Phys. Chem.* **1993**, *97*, 6859−6866.
(39) Leinweber, P.; Kruse, J.; Walley, F. L.; Gillespie, A.; Eckhardt, K.-U.; Blyth, R. I. R.; Regier, T. Nitrogen K-Edge XANES − an Overview of Reference Compounds Used to Identify 'Unknown' Organic Nitrogen in Environmental Samples. *J. Synchrotron Radiat.* **2007**, *14*, 500−511.
(40) Vinogradov, A. S.; Preobrajenski, A. B.; Molodtsov, S. L.; Krasnikov, S. A.; Szargan, R.; Knop-Gericke, A.; Hävecker, M. Nitrogen and Oxygen Core Excitations in Solid $NaNO_2$ Studied by X-ray Absorption and Resonant Photoemission. *Chem. Phys.* **1999**, *249*, 249−258.
(41) de Simone, M.; Coreno, M.; Alagia, M.; Richter, R.; Prince, K. C. Inner Shell Excitation Spectroscopy of the Tetrahedral Molecules CX4 (X = H, F, Cl). *J. Phys. B: At., Mol. Opt. Phys.* **2002**, *35*, 61−75.
(42) Feyer, V.; Plekan, O.; Tsud, N.; Cháb, V.; Matolín, V.; Prince, K. C. Adsorption of Histidine and Histidine-Containing Peptides on Au(111). *Langmuir* **2010**, *26*, 8606−8613.
(43) Newbury, D. C.; Ishii, I.; Hitchcock, A. P. Inner Shell Electron-Energy Loss Spectroscopy of Some Heterocyclic Molecules. *Can. J. Chem.* **1986**, *64*, 1145−1155.

DOI: 10.1021/acs.jpca.5b05950
J. Phys. Chem. A XXXX, XXX, XXX−XXX